JOURNAL OF THERMOPHYSICS AND HEAT TRANSFER
Vol. 20, No. 3, July–September 2006

Technical Notes

TECHNICAL NOTES are short manuscripts describing new developments or important results of a preliminary nature. These Notes should not exceed 2500 words (where a figure or table counts as 200 words). Following informal review by the Editors, they may be published within a few months of the date of receipt. Style requirements are the same as for regular contributions (see inside back cover).

Transient Thermal Effects of Radiant Energy in Semitransparent Materials

Parham Sadooghi*
K.N.T University of Technology, 1998743781 Tehran, Iran

Nomenclature

D = thickness of the medium, m
$E_1 \cdots E_n$ = exponential integral functions,

$$E_n(x) = \int_0^1 [\mu^{n-2} - \exp(-x/\mu)\,\mathrm{d}\mu]$$

k = thermal conductivity of the medium, W/m-K
M = number of increments in the X direction
N = conduction-radiation parameter, $k/4\sigma T_i^4 D$
n = refractive index of the medium
Q = incidence radiation, W/m^2
q_1, q_2 = radiosity from the interior of the two boundaries, W/m^2
$\bar{q}_1, \bar{q}_2$ = dimensionless radiosities, $q_1/\sigma T_i^4$, $q_2/\sigma T_i^4$
R = dimensionless gradient of radiative heat flux
S = source function
T = absolute temperature, K
T_e = temperature of the surroundings, K
T_i = initial temperature, K
T_m = mean temperature, K
t = dimensionless temperature, T/T_i
t_m = dimensionless mean temperature, T_m/T_i
t^* = temperature from the previous iteration
X = dimensionless coordinate, x/D
x = coordinate in direction across the layer, m
α = absorption coefficient of the layer, m^{-1}
β = extinction coefficient of the layer, m^{-1}
θ = time, s
κ_D = optical thickness of the layer, βD
ρ = interface reflectivity
ρC_P = product of density and specific heat of the layer, q/m^3 − K
σ = stefan–Boltzmann constant
τ = dimensionless time $(4\sigma T_i^4/\rho C_P D)\theta$
ϕ = dimensionless incident radiation, $Q/\sigma T_I^4$
ω = scattering albedo

Introduction

FIBER-REINFORCED composite materials are now an important class of engineering materials. Because of their useful properties, they are widely used in various fields of engineering. They offer outstanding mechanical properties, unique flexibility in design capabilities, and ease of fabrication. Additional advantages include light weight, corrosion resistance, impact resistance, and excellent fatigue strength. Today, fiber composites are routinely used in such diverse applications as automobiles, aircraft, plastic industries,[1] space vehicles, off–shore structures, containers and piping, sporting goods, electronics, and appliances.

The need for high-temperature reinforcing fibers has led to the development of ceramic fibers. An important factor that limits the performance (efficiency and emission) of current gas turbines is the temperature handling capability (strength and durability) of the metallic structural components in the engine hot section (blades, nozzles, vanes, and combustor liners). It is generally agreed that the temperature handling capabilities of metals have reached their ceiling. Ceramic fibers such as alumina fibers and silicon-carbide fibers exhibit superior durability and combine high strength and elastic modulus with high temperature capability, which implies their potential to revolutionize gas-turbine technology.

Accurate prediction of temperature distributions in ceramic and other fibrous and semitransparent materials (STM) at high temperature is essential during various fabrication operations. Within a semitransparent medium, the temperature and heat-flux distributions are affected by radiation in addition to heat conduction.[2–4] The transient coupled radiative and conductive heat transfer in a semitransparent medium is one of the pervasive processes in engineering applications, such as heat-dissipating materials, tempered glass and the application of its products,[5–9] thermal property analysis for ceramic parts,[10] manufacture and application of optical fibers and their products,[11] melting and removal of ice layers,[12] transient response to volumetrically scattering heat shields,[13,14] and ignition and flame spread for translucent plastics and solid fuels. Radiation effects become more important when STM are at elevated temperatures, are in high-temperature surroundings, or are subjected to large incident radiation and the radiative fluxes depend strongly on the temperature level. In semitransparent materials where thermal radiation can affect internal temperature distribution, transient behavior has been studied much less than steady-state behavior.

To obtain transient solutions, numerical procedures such as finite difference, finite element, and discrete ordinates methods have been used to solve the radiative-transfer equation coupled with the transient energy equation. The transient thermal behavior of single and multiple layers of semitransparent materials has been studied for a variety of cases, as reviewed recently by Siegel.[15]

Earlier studies concerning transient coupled radiative-conductive heat transfer in STM were carried out mainly for boundary conditions of the first kind, with prescribed temperatures at the boundaries. They were summarized by Viskanta and Anderson.[16] Much research has been directed toward the combined effects of conduction and radiation in glass. Chui and Gardon[17] undertook the study of combined conduction and radiation in gray glass. Su and Sutton[18] predicted temperatures and heat fluxes with 16 spectral bands in a silica glass plate externally heated by a constant heat input at one boundary for a 5-s time interval. Siegel,[19] and more recently Sadooghi and Aghanajafi,[2] used finite difference procedures to predict transient temperature distributions in a semitransparent material with a refractive index of one. Problems were also solved for refractive indices larger than one, which provided internal reflection. Hahn and Raether[20] examined transient heat transfer in a layer of

Received 27 March 2005; revision received 3 November 2005; accepted for publication 3 November 2005.

*Professor, Mechanical Engineering Department; parhampari2002@yahoo.com.

ceramic powder during laser-flash measurements of thermal diffusivity. A three-flux method was used to solve the radiative-transfer equation. However, no results were presented on the effect of scattering or refractive indices. The solution of the exact radiative equation is rather complicated, particularly when scattering is present; hence, a common approach is to use approximate methods such as the two-flux diffusion and differential approximation methods. Unfortunately, approximate methods are usually subject to certain constraints. Thus under certain conditions, some methods might not be valid. This paper presents a direct numerical procedure for obtaining accurate transient temperature distributions in a layer of semitransparent material. The solution includes the integral equation for the radiative flux gradient, coupled to a transient energy equation that contains both radiative and conductive terms. Solutions are given to demonstrate the effect of isotropic scattering on the radiative cooling of the layer.

Analysis

The analysis is for a gray absorbing, emitting, isotropically scattering, and heat-conducting layer of thickness D, as shown in Fig. 1. Initially the layer is at a uniform temperature T_i. It is then placed in much colder surroundings. The transient energy equation in dimensionless form is[21]

$$\frac{\partial t}{\partial \tau} = N\frac{\partial^2 t}{\partial X^2} - R(t) \tag{1}$$

where $R(t)$ is the gradient of the radiative flux under the assumption of isotropic scattering and is a function of X and τ:

$$R(t) = \kappa_D(1-\omega)\,[n^2t^4 - (\phi/4)] \tag{2}$$

where ϕ is the local incident radiation. Considering isotropic scattering, ϕ is given by[21]

$$\phi(X) = 2\bar{q}_1 E_2(\kappa_D X) + 2\bar{q}_2 E_2[\kappa_D(1-X)] + 2\pi\kappa_D\int_0^1 S(X')E_1(\kappa_D|X-X'|)\,\mathrm{d}X' \tag{3}$$

where the source function $S(X)$ is written as follows:

$$S(X) = (1-\omega)\,(n^2t^2) + (\omega/4\pi)\phi \tag{4}$$

where $\bar{q}_1$ and $\bar{q}_2$ are dimensionless diffuse fluxes at the boundaries $X = 0$ and 1, respectively. For the symmetric case, under the assumption of diffuse reflection,[22] and using Fresnel's reflective relations, $\bar{q}_1$ and $\bar{q}_2$ are given by

$$\bar{q}_1 = \bar{q}_2 = 2\pi\rho\kappa_D\int_0^1 [S(X')\,E_2(\kappa_D X')\,\mathrm{d}X']\,[2\rho E_3(\kappa_D)]^{-1} \tag{5}$$

Inserting Eqs. (4) and (5) into Eq. (3) leads to

$$\phi(X) = n^2\int_0^1 F(X,X')\,t^4(X')\,\mathrm{d}X' + 2n^2\kappa_D(1-\omega)\times\int_0^1 t^4(X')E_1(\kappa_D|X-X'|)\,\mathrm{d}X' + \frac{\omega}{4(1-\omega)}\int_0^1 F(X,X')\,\phi(X')\,\mathrm{d}X' + \frac{\omega}{2}\kappa_D\int_0^1 \phi(X')E_1(\kappa_D|X-X'|)\,\mathrm{d}X' \tag{6}$$

where

$$F(X,X') = 4\frac{\rho\kappa_D(1-\omega)}{1-2\rho E_3(\kappa_D)}\{E_2(\kappa_D X) + E_2[\kappa_D(1-X)]\}E_2(\kappa_D X') \tag{7}$$

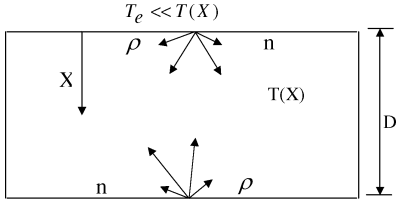

Fig. 1 Geometry and nomenclature of the plane layer.

Boundary Conditions

Because convective heat transfer is negligible, boundary conditions are required for radiation and for heat conduction only. Radiation passes out of the layer from within the material. There is no emission at the boundaries, which are planes without volume.[23] The energy is then lost only by means of internal radiation passing through the surface. There is no external conduction or convection, as in the case of a device used for dissipating waste heat from equipment operating in the cold vacuum of outer space. Therefore the following boundary conditions should be used for energy equation (1):

$$\frac{\partial t(0,\tau)}{\partial X} = \frac{\partial t(1,\tau)}{\partial X} = 0 \tag{8}$$

The initial temperature of the layer is uniform, and so the nondimensionalized temperature is initially equal to unity:

$$t(X,0) = 1 \tag{9}$$

Numerical Solution Procedure

The discretization of the energy equation is derived using an implicit finite volume scheme,[24]

$$R(t) = R(t^*) + \frac{\mathrm{d}R(t^*)}{\mathrm{d}t}(t-t^*) = R(t^*) - \frac{\mathrm{d}R(t^*)}{\mathrm{d}t}t^* + \frac{\mathrm{d}R(t^*)}{\mathrm{d}t}t \tag{10}$$

where t^* is temperature from the previous iteration. From Eq. (2), the time derivative of $R(t)$ in Eq. (10) is

$$\frac{\mathrm{d}R(t^*)}{\mathrm{d}t} = \kappa_D(1-\omega)\left(4n^2t^{*3} - \frac{1}{4}\frac{\mathrm{d}\phi^*}{\mathrm{d}t}\right) \tag{11}$$

and Eq. (6) gives

$$\frac{\mathrm{d}\phi^*(X)}{\mathrm{d}t} = 4n^2\int_0^1 F(X,X')\,t^{*3}(X')\,\mathrm{d}X' + 8(1-\omega)n^2\kappa_D\int_0^1 t^{*3}(X')E_1(\kappa_D|X-X'|)\,\mathrm{d}X' + \frac{\omega}{4(1-\omega)}\int_0^1 F(X,X')\frac{\mathrm{d}\phi^*(X')}{\mathrm{d}t}\,\mathrm{d}X' + \frac{\omega\kappa_D}{2}\int_0^1 \frac{\mathrm{d}\phi^*(X')}{\mathrm{d}t}E_1(\kappa_D|X-X'|)\,\mathrm{d}X' \tag{12}$$

By solving Eqs. (11) and (12), $\mathrm{d}R(t^*)/\mathrm{d}t$ is obtained.

Integral Eqs. (6) and (12) are solved numerically by using the well-known Nystrom method.[24] The layer is divided into M increments in the X direction with a smaller ΔX near the boundaries. The discretization of integral Eqs. (6) and (12) is derived using Gaussian quadrature.[20] Variable time increments are used with smaller time steps at the beginning of the process. At each time step, Eqs. (1), (2), (6), (11), and (12) are solved simultaneously, and iterations are performed to obtain the temperature distribution. For a solution at each time increment, an initial guess of the temperature distribution across the layer must be provided. Typically in this calculation, the temperature distribution at the previous time step is used for

the first guess. The values of temperature at the Gaussian abscissas are obtained using cubic spline interpolation.[25] With temperature specified, the values of R and dR/dt are obtained from the solution of Eqs. (2), (3), (11), and (12). The exponential integral function E_3 and values of R and dR/dt are then calculated using Nystrom interpolation.[25] With R and dR/dt evaluated, an updated temperature distribution is obtained by the solution of Eq. (1) in order to move ahead one time increment. The new temperature distribution is used to reevaluate the values of R and dR/dt. This process is repeated until the desired convergence is achieved. It is found that the larger the optical thickness of the layer, denser grids and higher-order Gaussian quadrature are needed because of steep variations in the radiative flux at the boundaries.

Results and Discussion

The effect of variation in the influence parameters, such as refractive index, optical thickness, and scattering albedo, on the temperature distributions are shown in Figs. 2–7. The conditions are symmetric, on both sides of the layer, and so the transient temperatures are symmetric, and the distributions are given for one–half of the layer. Results are given at three instances during the transient.

Figure 2 gives transient temperatures for a layer of $n = 1$ and Fig. 3 for $n = 1.5$ with $\omega = 0.3, 0.6$, and 0.9 for all figures. Different optical thicknesses and radiation–conduction parameters are considered. The results show that heat conduction serves to equalize temperature across the layer, and increased optical thickness makes the layer optically thick and gives a steeper temperature distribution near the boundaries. An important effect of a larger refractive index is that internal reflections promote the distribution of radiative energy within the layer. This makes the transient temperature distributions more uniform.

Figures 2 and 3 show the effect of scattering when the optical thickness is fixed. Increased scattering gives a more uniform temperature distribution and slows down the temperature drop. This is because of the layers relatively reduced ability to emit (or absorption thickness αD) when ω is increased. The radiative heat loss of the layer depends strongly upon the magnitude of αD, which is equal to $(1 - \omega)\kappa_D$. In this case, the effect of αD is somewhat similar to that of κ_D on a nonscattering layer. In the limiting case when

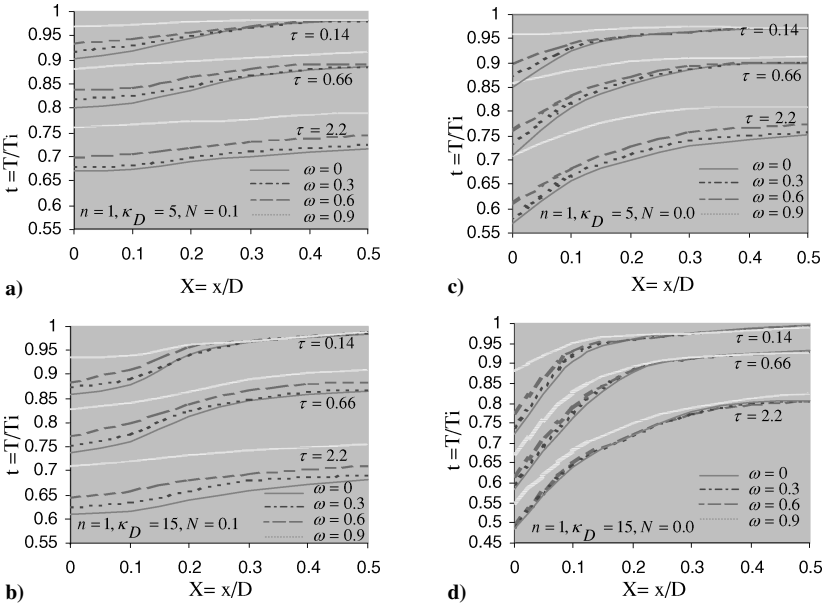

Fig. 2 Transient temperature distribution under various conditions for a layer with a) $n = 1, N = 0.1, \kappa_D = 5$; b) $n = 1, N = 0.1, \kappa_D = 15$; c) $n = 1, N = 0, \kappa_D = 5$; and d) $n = 1, N = 0, \kappa_D = 15$.

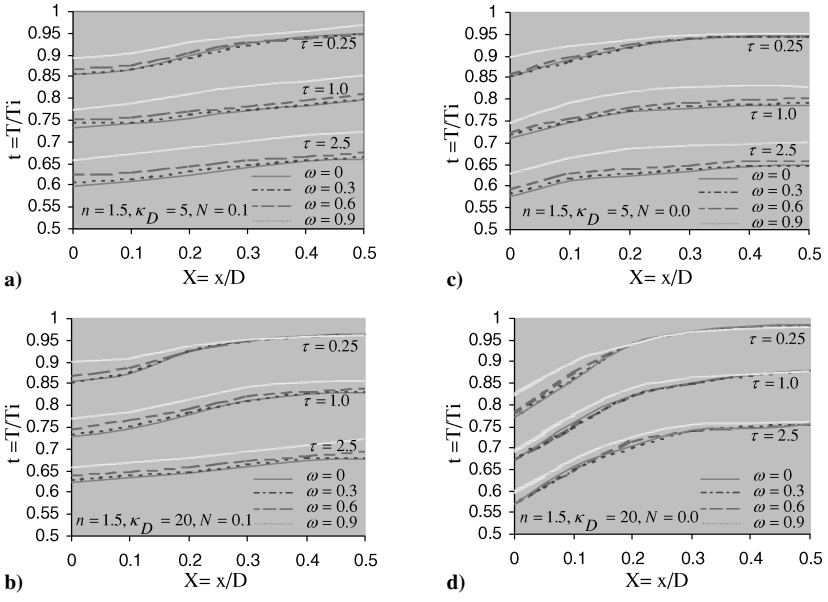

Fig. 3 Transient temperature distribution under various conditions for a layer with a) $n = 1.5, N = 0.1, \kappa_D = 5$; b) $n = 1.5, N = 0.1, \kappa_D = 20$; c) $n = 1.5, N = 0, \kappa_D = 5$; and d) $n = 1.5, N = 0, \kappa_D = 20$.

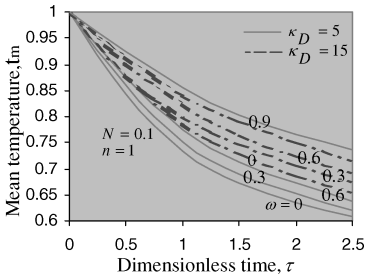

Fig. 4 Transient mean temperature of the layer of $n = 1$ with $N = 0.1$, $\kappa_D = 5$, and $\kappa_D = 15$.

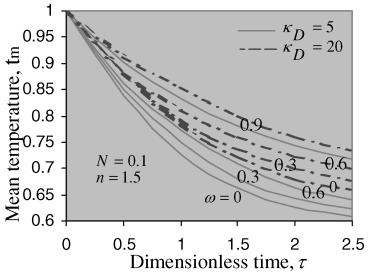

Fig. 5 Transient mean temperature of the layer of $n = 1.5$ with $N = 0.1$, $\kappa_D = 5$, and $\kappa_D = 20$.

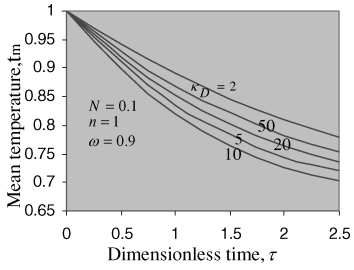

Fig. 6 Transient mean temperature of the layer of various κ_D at $\omega = 0.9$ for $n = 1$, $N = 0.1$.

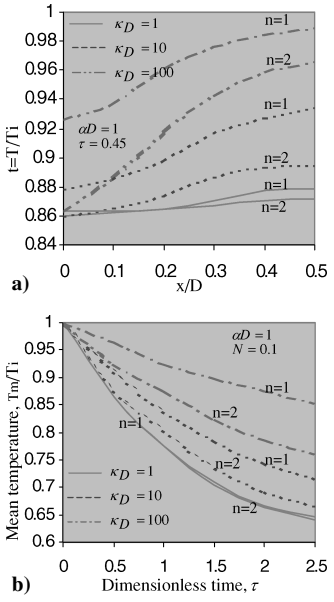

Fig. 7 Effect of increasing scattering with fixed $\alpha D = 1$ for $n = 1$ to 2 and $N = 0.1$: a) temperature distribution at $\tau = 0.45$ and b) transient mean temperature of the layer.

$\omega = 1$, the layer remains at the initial temperature because there is no emission or absorption, and hence no heat loss from the layer. The effect of increasing scattering albedo is significant for lower optical thickness. Comparison between parts a and b and between parts c and d in Figs. 2 and 3 shows that a larger optical thickness tends to weaken the effect of scattering. In this case, the reason is that a larger optical thickness and thus a larger absorption thickness means more scattered energy is absorbed, which offsets the effect of scattering.

The transient mean temperatures are shown in Fig. 4 (for $n = 1$) and Fig. 5 (for $n = 1.5$). The results show that, with other conditions kept constant as in parts a and b of Figs. 2 and 3, increasing scattering or decreasing the value of αD slows down the temperature decrease particularly at larger scattering albedos.

The fact that a larger optical thickness weakens the effect of scattering can be shown from Fig. 4. The difference between the curve corresponding to $\omega = 0$ and the curve corresponding to $\omega = 0.9$ for $\kappa_D = 5$ is larger than that for $\kappa_D = 15$, at any time and at any temperature level. Figure 4 shows that the curve corresponding to $\kappa_D = 5$, $\omega = 0.9$ lies above the curve corresponding to $\kappa_D = 15$, $\omega = 0.9$. The effect of large scattering is shown in Fig. 6. The scattering albedo is held constant at $\omega = 0.9$, but the optical thickness of the layer is varied from 2 to 50. At small values of optical thickness $\kappa_D < 10$, the transient mean temperature decreases with increasing optical thickness. However at larger κ_D, this trend is reversed. This is related to the magnitude of αD. When αD is small, the temperature distribution is relatively uniform, and the radiation rays pass out of the layer because of relatively small absorption. In this case, increasing αD enhances the radiation and hence the cooling rate. On the other hand, when κ_D is large, the temperature near the boundaries becomes increasingly cooler than the interior, if the heat conduction is finite, thus reducing the cooling effectiveness of the layer. This explains the special case appearing in Fig. 4 that was mentioned earlier. At such small αD, the cooling effectiveness increases with increasing αD and also by increased absorption.

In Fig. 7 the effect of scattering is shown in a different way. αD is held constant, while κ_D is increased such that the effect of additional scattering can be shown. The temperature distribution at $\tau = 0.45$ is shown in Fig. 7a. It is seen that increasing the scattering leads to a steeper temperature distribution near the boundaries, an observation different from that shown in Figs. 2 and 3. Note that in the case of Fig. 7 κ_D is increased much faster than the increase of ω. Thus the layer quickly becomes increasingly opaque. In contrast, in Figs. 2 and 3, κ_D is held constant when the effect of increased scattering is examined. Figure 7b reflects that the cooling rate of the layer decreases with increasing ω and κ_D, while αD is fixed. This is caused by the temperature distribution depicted in Fig. 7a.

Note the effect of refractive index on the transient process at large scattering albedos. In Figs. 2, 3, and 7, when $\omega = 0$, a larger n gives more uniform temperatures. At $N = 0.1$ and with κ_D ranging from 2 to 20, there is a decrease in the cooling rate when n is increased. However the effect of n is quite different at large ω as is shown in Fig. 7. When $\omega = 0.9$ and 0.99, the cooling rate with $n = 2$ is considerably faster than that for $n = 1$, and at $\kappa_D = 100$, $\omega = 0.99$ the temperature distribution for $n = 2$ is steeper than that for $n = 1$. This is most likely a result of enhanced cooling at positions near the boundary by a combined effect of strong scattering and interface reflection.

Conclusions

Transient solutions were obtained for an emitting, absorbing, isotropically scattering, and heat-conducting layer of a semitransparent material. The solution procedure includes simultaneously solving the transient energy equation using an implicit finite volume scheme and the integral equation for the radiative heat flux using the singularity subtraction technique and Gaussian numerical quadrature. The effects of influence parameters, optical thickness, scattering albedo, and refractive index of the layer are considered carefully. Scattering is found to have a significant effect on the transient temperature distributions of a layer subject to radiative cooling.

References

[1]Sadooghi, P., "Transient Combined Radiation and Conduction Heat Transfer in Plastics," *Journal of Vinly and Additive Technology*, Vol. 11, No. 1, 2005, pp. 28–36.

[2]Sadooghi, P., and Aghanajafi, C., "Coating Effects on Transient Cooling a Hot Spherical Body," *Journal of Fusion Energy*, Vol. 22, No. 1, 2004, pp. 59-65.

[3]Sadooghi, P., and Aghanajafi, C., "Radiation Effects in a Ceramic Layer," *Journal of Radiation Effects and Defects in Solids*, Vol. 159, No. 1, 2004, pp. 61–71.

[4]Sadooghi, P., "Transient Coupled Radiative and Conductive Heat Transfer in a Semitransparent Layer of Ceramic," *Journal of Quantitative Spectroscopy and Radiative Transfer*, Vol. 92, No. 4, 2005, pp. 403–416.

[5]Kunc, T., Lallemand, M., and Saulnier, J. B., " Some New Developments on Coupled Radiative-Conductive Heat Transfer in Glasses-Experiments and Modeling," *International Journal of Heat and Mass Transfer*, Vol. 27, No. 12, 1984, pp. 2307–2319.

[6]Field, R. E., and Viskanta, R., "Measurement and Prediction of the Dynamic Temperature Distributions in Soda Lime Glass Plates," *Journal of the American Ceramic Society*, Vol. 73, No. 7, 1990, pp. 2047–2053.

[7]Ducharme, R., Kapadia, P., Scarfe, F., and Dowden, J., "A Mathematical Model of Glass Flow and Heat Transfer in a Platinum Downspout," *International Journal of Heat and Mass Transfer*, Vol. 36, No. 7, 1993, pp. 1789–1797.

[8]Tan, H. P., and Lallemand, M., "Transient Radiative Conductive Heat Transfer in Flat Glasses Submitted to Temperature, Flux and Mixed Boundary Conditions," *International Journal of Heat and Mass Transfer*, Vol. 32, No. 5, 1989, pp. 795–810.

[9]Tan, H. P., Ruan, L. M., and Xia, X. L., "Transient Coupled Radiative and Conductive Heat Transfer in a Absorbing, Emitting and Scattering Media," *International Journal of Heat and Mass Transfer*, Vol. 42, No. 15, 1999, pp. 2967–2980.

[10]Thomas, J. R., "Coupled Radiation-Conduction Heat Transfer in Ceramic Liners for Diesel Engines," *Numerical Heat Transfer*, Vol. 21, No. 1, 1992, pp. 109–120.

[11]Yin, Z., and Jaluria, Y., "Zonal Method to Model Radiative Transport in an Optical Fiber Drawing Furnace," *Journal of Heat Transfer*, Vol. 119, No. 2, 1997, pp. 597–603.

[12]Song, B., and Viskanta, R., "Deicing of Solids Using Radiant Heating," *Journal of Thermophysics and Heat Transfer*, Vol. 4, No. 3, 1993, pp. 311–317.

[13]Howe, J. T., and Yang, L., "Earth Atmosphere Entry Thermal Protection by Radiation Backscattering Ablating Materials," *Journal of Thermophysics and Heat Transfer*, Vol. 7, No. 1, 1993, pp. 74–81.

[14]Cornelison, C. J., and Howe, J. T., "Analytic Solution of the Transient Behavior of Radiation Backscattering Heat Shields," *Journal of Thermophysics and Heat Transfer*, Vol. 6, No. 4, 1992, pp. 612–617.

[15]Siegel, R., "Transient Thermal Effects of Radiant Energy in Translucent Materials," *Journal of Heat Transfer*, Vol. 120, No. 1, 1998, pp. 4–20.

[16]Viskanta, R., and Anderson, E. E., "Heat Transfer in Semitransparent Solids," *Advances in Heat Transfer*, Vol. 11, No. 1, 1975, pp. 317–441.

[17]Chui, G. K., and Gardon, R., "Interaction of Radiation and Conduction in Glass," *Journal of the American Ceramic Society*, Vol. 52, No. 2, 1969, pp. 548–553.

[18]Su, M. H., and Sutton, W. H., "Transient Conductive and Radiative Heat Transfer in a Silica Window," *Journal of Thermophysics and Heat Transfer*, Vol. 9, No. 1, 1995, pp. 370–373.

[19]Siegel, R., "Refractive Index Effects on Transient Cooling of a Semitransparent Radiating Layer," *Journal of Thermophysics and Heat Transfer*, Vol. 9, No. 1,1995, pp. 55–62.

[20]Hahn, O., and Raether, F., "Transient Coupled Conductive-Radiative Heat Transfer in Absorbing, Emitting and Scattering Media," *International Journal of Heat and Mass Transfer*, Vol. 40, No. 3, 1997, pp. 689–697.

[21]Siegel, R., and Howell, J. R., *Thermal Radiation Heat Transfer*, 3rd ed., Hemisphere, Washington, DC, 1992, Chap. 14.

[22]Spuckler, C. M., and Siegel, R., "Refractive Index and Scattering Effects on Radiative Behavior of a Semitransparent Layer," *Journal of Thermophysics and Heat Transfer*, Vol. 7, No. 2, 1993, pp. 303–310.

[23]Siegel, R., "Finitte Difference Solution for Transient Cooling of a Radiating-Conducting Semitransparent Layer," *Journal of Thermophysics and Heat Transfer*, Vol. 6, No. 6, 1999, pp. 77–83.

[24]Patankar, S. V., *Numerical Heat Transfer and Fluid Flow*, Hemisphere, Washington, DC, 1992, Chap. 2.

[25]Press, W. H., Teukolsky, S. A., Vetterling, T. W., and Flannery, B. P., *Numerical Recipes in Fortran*, 2nd ed., Cambridge Univ. Press, New York, 1992, Chap. 3.